# Simultaneous analysis of near-barrier elastic scattering and fusion of $^{9}$Be with $^{27}$Al

A. Gómez Camacho*
*Departamento de Aceleradores Instituto Nacional de Investigaciones Nucleares Apartado Postal 18-1027, C.P. 11801, México, D.F., Mexico*

P. R. S. Gomes and J. Lubian
*Instituto de Fisica, Universidade Federal Fluminenese Avenida Litoranea s/n, Gragoatá, Niterói RJ 24210-340, Brazil*

L. F. Canto
*Instituto de Física, Universidade Federal do Rio de Janeiro C.P. 68528, Rio de Janeiro, RJ 21941-972, Brazil*
(Received 3 May 2010; published 26 July 2010)

A simultaneous analysis of elastic scattering and fusion of the weakly bound projectile $^{9}$Be with the light deformed $^{27}$Al target,at energies close to the Coulomb barrier, is carried out by optical model calculations. The nuclear polarization potential $U$ is split into a volume part $U_F$, which accounts for fusion reactions and a surface part $U_{\rm DR}$, responsible for the direct reactions. The presence of the threshold anomaly in the elastic scattering is investigated. We also estimate the distance where breakup starts to occur. The present results are compared with those for the same projectile on the medium size and spherical $^{144}$Sm target, to investigate the effect of the Coulomb breakup and target deformation in the behavior of the elastic scattering.

DOI: 10.1103/PhysRevC.82.014616 PACS number(s): 25.70.Bc, 24.10.Ht, 25.70.Jj, 27.20.+n

## I. INTRODUCTION

The influence of the breakup of weakly bound nuclei on near-barrier elastic scattering and fusion is presently a subject of great interest [1]. The effects of breakup may vary at different energy regimes (below and above the Coulomb barrier) and with the target charge, due to the Coulomb breakup.

A long time ago, it was shown that for reactions with heavy and tight nuclei, the real and imaginary parts of the optical potential slowly depend on the energy at the above energy regime. However, as the energy is lowered toward the Coulomb barrier, the imaginary part of the optical potential sharply decreases while the real part presents a localized peak. This phenomenon, known as the threshold anomaly [2], is a manifestation of the physical concept of causality, which states that no reaction occurs before the incident wave reaches the scattering center. The mathematical connection between the energy dependent real and imaginary parts of the optical potential $U(E) = V(E) + iW(E)$ is the dispersion relation which is given by [3,4]

$$V(E) = V(E_s) + (E - E_s)\frac{1}{\pi}\mathcal{P}\int_0^\infty \frac{W(E')}{(E' - E_s)(E' - E)}dE', \tag{1}$$

where $V(E_s)$ is the value of the potential at the reference energy $E_s$. The threshold anomaly may be ascribed to the coupling of the elastic scattering to other reaction channels that produces an attractive polarization potential $V(E)$, that in turn leads to a net enhancement of the sub-barrier fusion cross section, due to the lowering of the Coulomb barrier. On the other hand, the behavior of the imaginary potential is related to the closing of nonelastic peripheral channels at energies near and below the barrier.

In contrast, the situation is different when reactions with weakly bound projectiles are considered. Here, at energies around and even below the Coulomb barrier, large breakup cross sections have been measured. Indeed, breakup cross sections are larger than fusion ones at these energies have been observed [5–7]. Therefore, to account for the nondiminishing coupling to the breakup channel, the imaginary part of the optical potential can not decrease around the Coulomb barrier as in the case of tightly bound nuclei. As a consequence, the corresponding real part of the optical potential presents a net repulsive character that is produced mainly by the couplings to the continuum breakup states [8–12]. Owing to the combined effect between the real and imaginary parts of the dynamic polarization potential, the usual threshold anomaly may not be present in reactions with weakly bound projectiles. This effect is called the breakup threshold anomaly (BTA) [13] to emphasize that it arises from the coupling to the breakup channel.

This BTA has been observed in several systems involving weakly bound stable projectiles like $^{6,7}$Li and $^{9}$Be [13–16]. Also, the BTA has been observed in the nuclear optical potential of the halo $^{6}$He projectile impinging on heavy targets $^{209}$Bi [17] and $^{208}$Pb [18] at near barrier energies. Recent calculations [19] about the threshold anomaly for the nuclear systems $^{8}$B, $^{7}$Be, and $^{6}$Li on the target $^{58}$Ni using the data of Aguilera *et al.* [20] show that two independent dynamic polarization potentials, namely, the density dependent double folding São Paulo potential and the Woods-Saxon potential with volume and surface parts suggest that in fact the BTA occurs.

One widely used approach to study the threshold anomaly is based on energy dependent Woods-Saxon potentials of the dynamic polarization potential [21,22], i.e.,

$$U_N(E, r) = U_F(E, r) + U_{\rm DR}(E, r), \tag{2}$$

where $U_F = V_F + iW_F$ is the fusion potential (responsible for fusion reactions) and $U_{\rm DR} = V_{\rm DR} + iW_{\rm DR}$ the direct reaction

*Corresponding author: arturo.gomez@inin.gob.mx

 

potential (responsible for direct reactions). These potentials have respectively volume and surface Woods-Saxon shapes, i.e., $V_F$ and $W_F$ have the same volume shape while $V_{\rm DR}$ and $W_{\rm DR}$ have the same surface shape. The parameters of these potentials are determined by a simultaneous fitting to elastic and fusion data and in order to minimize ambiguities, these potentials are calculated at the radius of sensitivity. The behavior of the fusion and direct reaction potentials as the energy approaches the Coulomb barrier can tell us if the TA or BTA shows up for a given nuclear system. It should be noticed that the pairs of potentials $V_F(E)$ and $W_F(E)$ as well as $V_{\rm DR}(E)$ and $W_{\rm DR}(E)$ of Eq. (2) obtained during the data fitting should be in accordance to the dispersion relation [3].

In this paper, the reactions of the weakly bound nucleus $^9$Be with the $^{27}$Al target are analyzed by means of the Woods-Saxon polarization potentials. A simultaneous calculation of the fusion excitation function and elastic scattering is performed. The basic purposes are to determine whether or not the threshold anomaly or breakup threshold anomaly appears and which is the distance where breakup starts to occur. We also investigate whether there are differences on these behaviors for light and heavy targets. For that comparison, we use the results obtained by us for the $^9$Be + $^{144}$Sm system [23,24].

The weakly bound nucleus $^9$Be has the property that when the valence neutron is knocked out, the remaining nucleus $^8$Be becomes unstable and decays into two $\alpha$ particles with $T_{1/2} = 0.07$ fs. Even more, $^9$Be is strongly deformed since its $^8$Be core has a well known $\alpha$-$\alpha$ structure. The breakup mechanism of $^9$Be can proceed through the channels $^9{\rm Be} \Rightarrow n + {}^8{\rm Be}$ with a threshold energy $E_{\rm th} = 1.665$ MeV or through $^9{\rm Be} \Rightarrow \alpha + {}^5{\rm He}$ with $E_{\rm th} = 2.467$ MeV. Now, since both $^8$Be and $^5$He are unbound, these decay channels end up in two $\alpha$ particles plus a neutron. In a nuclear reaction with $^9$Be several processes can occur after breakup: noncapture breakup (NCBU) occurs when none of the fragments are captured by the target, incomplete fusion (ICF) when one of the $\alpha$ particles fuses to the target, complete fusion (CF) when the whole projectile $^9$Be fuses to the target or when all the fragments after breakup fuse to the target and neutron transfer (NT) when the neutron produced after breakup is transferred to the outer shells of the target. Total fusion (TF) is the sum CF + ICF.

For the $^9$Be + $^{27}$Al system, the analysis is performed using the elastic scattering angular distributions and fusion cross sections of Refs. [25,26]. Previously, elastic scattering angular distributions for the $^9$Be + $^{27}$Al system were analyzed using the double-folding São Paulo potential [25]. In this paper, a nearly energy independent optical potential was derived. This was an indication that around the barrier there is a contribution from a repulsive potential that arises from coupling to breakup channel of $^9$Be. So, the effect of this repulsive polarization potential is to compensate the attractive polarization potential due to inelastic target excitations [11,27]. From the results for the behavior of the real and imaginary with the energy of Refs. [25,26], it was concluded that the system $^9$Be + $^{27}$Al presents the so-called BTA. In this work, we intend to corroborate this conclusion by the use of Woods-Saxon polarization potentials as indicated above. This is investigated by determining the energy dependence of the real and imaginary potentials around the Coulomb barrier which is found from a simultaneous fitting of elastic scattering angular distributions and fusion cross sections. Also, by studying the radial behavior of the imaginary fusion and direct reaction polarization potentials $W_F(E, r)$ and $W_{\rm DR}(E, r)$ around the sensitivity region, we find that not only the condition $|W_F| < |W_{\rm DR}|$ is satisfied but also where indeed the breakup of $^9$Be starts to occur. In this regard, we compare our findings to those obtained for the $^9$Be + $^{144}$Sm reaction [23,24] in order to analyze where the breakup process starts in reactions with the same projectile but with a more massive and spherical target as $^{144}$Sm.

## II. CALCULATIONS AND RESULTS

The parameters of the volume potentials $V_F$ and $W_F$ are adjusted to the total fusion data [26] while the corresponding parameters of the surface potentials $V_{\rm DR}$ and $W_{\rm DR}$ are determined to fit the direct reaction cross sections $\sigma_{\rm DR} = \sigma_R - \sigma_{\rm TF}$, where $\sigma_R$ is the total reaction cross section derived from the elastic scattering data [25]. It is assumed that for this nuclear system, incomplete fusion is negligible as compared to complete fusion in the whole range of energies considered in this work. As fusion data were not available at exactly the same energies as the elastic scattering data, smooth interpolation fusion cross section values were used.

If total absorption $W$ of Eq. (1) is written in terms of the fusion and direct reaction terms $W_F$ and $W_{\rm DR}$, i.e., $W = W_F + W_{\rm DR}$, then the corresponding real polarization potentials $V_F(E)$ and $V_{\rm DR}(E)$, arising from couplings to fusion and direct reaction channels are given by

$$V_i(r, E) = V(E_{s,i}) + (E - E_{s,i})\frac{1}{\pi}\mathcal{P} \times \int_0^\infty \frac{W_i(r, E')}{(E' - E_{s,i})(E' - E)} dE', \quad i = F, DR. \tag{3}$$

In our calculations, the parameters of the energy independent potential $V_0(r)$, as formulated in the model described in Refs. [21,22] are determined by fitting the elastic scattering angular distributions at the largest energy. These have been fixed at $V_0 = 60$ MeV, $r_0 = 1.22$ fm and $a_0 = 0.52$ fm. The fusion and direct reaction polarization potentials of Eq. (2) can be written as

$$U_{F,{\rm DR}}(E, r) = V_{F,{\rm DR}}(E, r) + i\, W_{F,{\rm DR}}(E, r). \tag{4}$$

The real fusion and direct reaction potentials $V_F$ and $V_{\rm DR}$ have the same geometrical shapes as their counterparts $W_F$ and $W_{\rm DR}$. For the sake of comparison, we fix the reduced radius of $W_F(E, r)$ at the same value as done in the case of $^9$Be + $^{144}$Sm [23], i.e., $r_F = 1.2$ fm. Now, during the simultaneous fitting of elastic scattering and fusion data, the reduced radius of $W_{\rm DR}(E, r)$, i.e., $r_{\rm DR}$ is varied from 1.4 fm to 2.0 fm leaving the potentials depths $W_F(E)$, $W_{\rm DR}(E)$ and the diffuseness $a_F$ and $a_{\rm DR}$ to be calculated by the $\chi^2$ fitting of the data. The simultaneous calculations to elastic and fusion cross sections data of Refs. [25,26], showed that in order to obtain fittings with reasonable low $\chi^2$ values to all collision energies and that the fusion and direct reaction imaginary potentials satisfy the constraint $|W_F| < |W_{\rm DR}|$, it

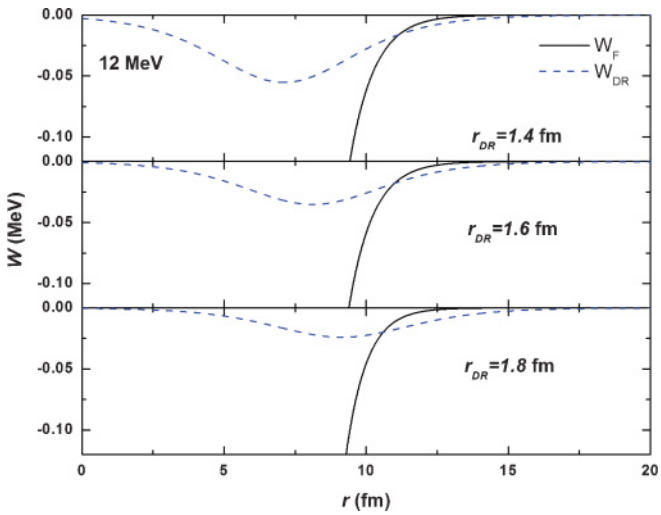


FIG. 1. (Color online) Radial dependence of the fusion $W_F$ and direct reaction $W_{\rm DR}$ imaginary polarization potentials for $E_{\rm lab} = 12$ MeV for the $^9$Be + $^{27}$Al system.

was necessary to assume large direct reaction diffuseness values, i.e., of the order $a_{\rm DR} = 1.64$ fm. So, we fix this value for all energies. Figure 1 shows the results for the lowest available energy $E_{\rm lab} = 12$ MeV for different $r_{\rm DR}$ values where $|W_F| < |W_{\rm DR}|$ is satisfied at the tail region of the potentials. In Fig. 2, the same calculations are shown for the $E_{\rm lab} = 40$ MeV collision energy. As observed, for values for $r_{\rm DR} = 1.6, 1.8$ fm, the condition $|W_F| < |W_{\rm DR}|$ is already satisfied at the tail region of the potentials. Fundamentally the condition $|W_F| < |W_{\rm DR}|$ means that direct reaction processes, basically breakup reactions, begin at distances larger than those where fusion starts to take place. Figures 1 and 2 show that this is clearly the case for values $r_{\rm DR} = 1.8$ and 2.0 fm. With the parameters shown in Table I, good fits for fusion and elastic scattering cross sections were obtained for all energies of Refs. [25,26] with $\chi^2$ values/point smaller than 1.5 With these

TABLE I. Calculated values for the optical potential parameters for $^9$Be + $^{27}$Al. Energy depths in MeV, diffuseness in fm.

| $E_{\rm c.m.}$ (MeV) | $V_{0,F}$ | $W_{0,F}$ | $V_{0,\rm DR}$ ($10^{-2}$) | $W_{0,\rm DR}$($10^{-2}$) | $a_F$ | $\chi^2/N$ |
|---|---|---|---|---|---|---|
| 9.0 | 28.0 | 5.0 | 2.4 | 2.5 | 0.72 | 0.25 |
| 10.5 | 29.2 | 12.0 | 1.9 | 2.2 | 0.70 | 1.2 |
| 13.5 | 23.9 | 17.1 | 1.1 | 2.6 | 0.72 | 0.97 |
| 16.5 | 18.8 | 27.6 | 0.9 | 2.0 | 0.70 | 0.49 |
| 18.75 | 5.6 | 13.4 | 0.7 | 1.7 | 0.77 | 1.3 |
| 21.0 | 17.0 | 26.5 | 0.8 | 1.8 | 0.70 | 0.9 |
| 24.0 | 2.0 | 15.4 | 0.8 | 1.9 | 0.78 | 1.5 |
| 24.75 | 1.8 | 12.1 | 0.8 | 1.8 | 0.78 | 0.2 |
| 26.25 | 4.2 | 26.5 | 0.5 | 2.5 | 0.70 | 0.5 |
| 30.0 | 1.3 | 8.3 | 0.5 | 1.7 | 0.81 | 0.7 |
| 35.25 | 1.2 | 7.9 | 0.6 | 1.8 | 0.81 | 0.12 |

parameters, similar conclusions regarding the region where breakup starts are achieved for all the energies considered.

The energy dependence of the real and imaginary polarization potentials evaluated at the radius of sensitivity $R_s = 12.1$ fm is given in Fig. 3, where the error bars are determined by calculating the range of variation of the potentials for a corresponding variation in $\chi^2/N$ in one unity. As seen in this figure the energy dependence of the fusion potentials $V_F(E)$ and $W_F(E)$ shows a behavior expected for the usual threshold anomaly around the Coulomb barrier $V_B$. The real potential $V_F(E)$ calculated from the dispersion relation Eq. (3) agrees very well with values obtained from the $\chi^2$ fitting. It should be noted that energy and potential reference values $E_{s,F} = 15$ MeV and $V(E_{s,F}) = 0.4$ MeV have been used. On the other hand, direct reaction potential $W_{\rm DR}(E)$ dominates over the fusion potential $W_F(E)$ in the whole energy region and presents an increase as the energy decreases toward the barrier $V_B$. The fitted values of $V_{\rm DR}(E)$ are also consistent with the results from the dispersion relation for which reference values $E_{s,\rm DR} = 9.0$ MeV and $V(E_{s,F}) = 1.0$ MeV are used.

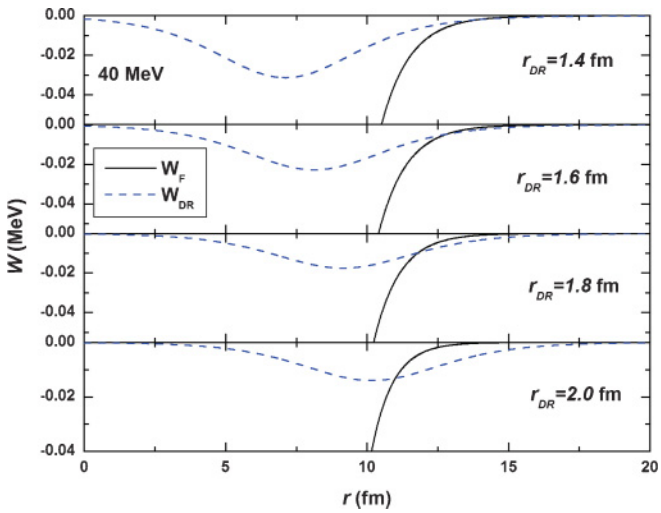


FIG. 2. (Color online) Radial dependence of the fusion $W_F$ and direct reaction $W_{\rm DR}$ imaginary polarization potentials for $E_{\rm lab} = 40$ MeV for the $^9$Be + $^{27}$Al system.

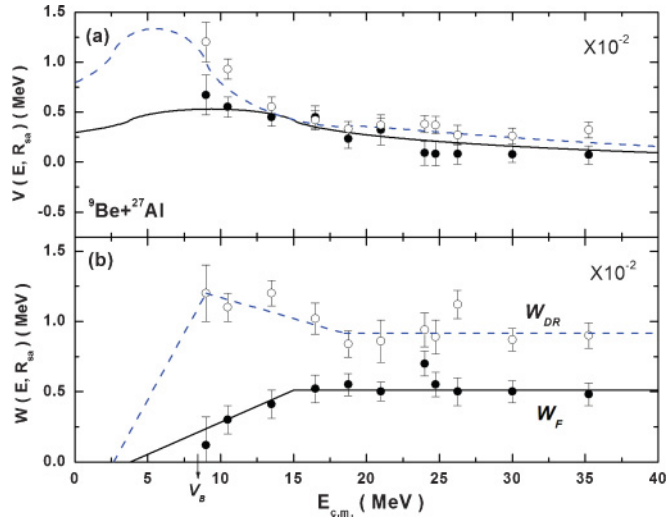


FIG. 3. (Color online) Energy dependence of the real ($V_F$, $V_{\rm DR}$) and imaginary ($W_F$, $W_{\rm DR}$) polarization potentials at the radius of sensitivity $R_s = 12.1$ fm for the nuclear system $^9$Be + $^{27}$Al.

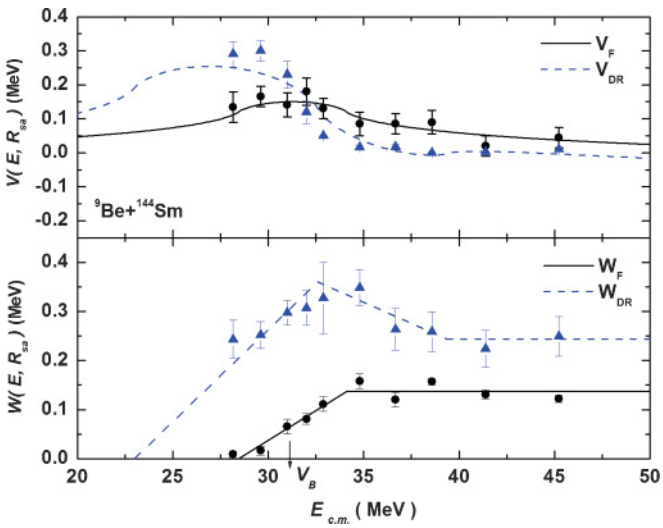


FIG. 4. (Color online) Energy dependence of the real ($V_F$, $V_{\rm DR}$) and imaginary ($W_F$, $W_{\rm DR}$) polarization potentials at the radius of sensitivity $R_s = 11.8$ fm for the nuclear system $^9$Be + $^{144}$Sm.

From this, we can conclude that the nuclear system $^9$Be + $^{27}$Al presents the breakup threshold anomaly.

As for the $^9$Be + $^{144}$Sm nuclear system, Fig. (11) of our earlier work [23] shows the energy dependence of the fusion and direct reaction imaginary polarization potentials $W_F(E)$ and $W_{\rm DR}(E)$ at the radius of sensitivity $R_s = 11.8$ fm. Thus, in Fig. 4 of the present work, we show the values of the real polarization potentials $V_F(E)$ and $V_{\rm DR}(E)$ as obtained from the simultaneous $\chi^2$ fitting of complete fusion and elastic scattering angular distributions. Also in this figure, the results of the dispersion relation calculations are presented as obtained from the linear parametrizations shown for $W_F(E)$ and $W_{\rm DR}(E)$. It is also observed in this figure that $W_{\rm DR}(E)$ does not seem to decrease around the barrier $V_B$ as the bombarding energy diminishes. This is so, since $W_{\rm DR}(E)$ must account for the appreciable breakup excitation function measured for this nuclear system at low energies as observed in Fig. (2) of Ref. [23]. Thus, the breakup threshold anomaly seems to be present also for the system $^9$Be + $^{144}$Sm.

We end this work with some discussion about the region where the breakup process starts to take place for both systems $^9$Be + $^{27}$Al and $^9$Be + $^{144}$Sm. As seen before in Figs. 1 and 2 for $^9$Be + $^{27}$Al at $E_{\rm lab} = 12$ MeV and 40 MeV (the situation was the same for the other energies), in order to obtain simultaneous fits to elastic and fusion cross sections with small $\chi^2$/point values, large diffuseness $a_{\rm DR} \sim 1.64$ fm, $a_F \sim 0.7$ fm with reduced radii $r_F = 1.2$ fm and $r_{\rm DR} = 1.8 - 2.0$ fm were required. Only with these values the restriction $|W_F| < |W_{\rm DR}|$ was satisfied at the tail region of the potentials. On the other hand, for the $^9$Be + $^{144}$Sm system, Figs. (12) and (13) of Ref. [23] and the discussion therein, show that with the same $r_F = 1.2$ fm, smaller diffuseness values $a_F \sim 0.65$ fm and $a_{\rm DR} \sim 0.7$ fm with reduced $r_{\rm DR} \sim 1.6$ fm were needed to satisfy $|W_F| < |W_{\rm DR}|$ at all the energies studied. From these results, it can be concluded that breakup reactions start at larger distances for $^9$Be + $^{27}$Al than for $^9$Be + $^{144}$Sm. Since the projectile in both cases is the same and the fact that smaller diffuseness values are needed for the case of $^9$Be + $^{144}$Sm tells that the $^{144}$Sm nucleus represents a more compact target than the highly deformed nucleus $^{27}$Al.

## III. SUMMARY

A simultaneous fitting of elastic scattering and fusion cross sections for the system $^9$Be + $^{27}$Al has been presented. In the calculations a volume and surface Woods-Saxon polarization potentials have been used to describe fusion and direct reaction cross sections respectively. In order to compare the results with those previously studied for a reaction with the same projectile $^9$Be and a more massive but spherical target like $^{144}$Sm, some optical potential parameters are chosen to be the same. As a matter of fact, the parameters are found in such a way that the condition $|W_F| < |W_{\rm DR}|$ must be satisfied. That is, that direct reactions must begin at distances larger than those where fusion reactions begin at the tail region. The simultaneous $\chi^2$ fitting of fusion and total reaction cross section data ($\sigma_{\rm DR} = \sigma_R - \sigma_F$) for $^9$Be + $^{27}$Al, indicate that direct reactions (basically breakup) start at slightly larger distances than those determined for the $^9$Be + $^{144}$Sm nuclear system. That is, the study of two reactions with the same projectile $^9$Be, the more massive $^{144}$Sm represents a more compact target than the highly deformed $^{27}$Al.

Also, in this work, the energy dependence of the real and imaginary parts of the fusion potential $U_F$ and direct reaction potential $U_{\rm DR}$ has been determined for the reaction $^9$Be + $^{27}$Al. It has been found that, at the sensitivity radius $R_s$, the real and imaginary parts of the potentials follow the dispersion relation. In fact, the fusion potentials $V_F(E)$ and $W_F(E)$ behave according to the well-known threshold anomaly. That is, $W_F(E)$ decreases as the energy approaches the barrier from higher energies and $V_F(E)$ has an increasing and decreasing behavior for energies around the barrier $V_B$. On the other hand, the direct reaction potential $W_{\rm DR}(E)$, besides dominating over $W_F(E)$ has an slight increasing tendency as the energy is lowered toward the barrier. The real $V_{\rm DR}(E)$ manifests a small repulsive character in this same energy region. This conjugated effect for the energy dependence of the polarization potentials indicate that the $^9$Be + $^{27}$Al system presents the so-called breakup threshold anomaly.

## ACKNOWLEDGMENTS

P.R.S.G., J.L., and L.F.C. acknowledge the financial support from CNPq, PRONEX, and FAPERJ.

[1] L. F. Canto, P. R. S. Gomes, R. Donangelo, and M. S. Hussein, Phys. Rep. **424**, 1 (2006).
[2] G. R. Satchler, Phys. Rep. **199**, 147 (1991).
[3] C. Mahaux, H. Ngô, and G. R. Satchler, Nucl. Phys. A **449**, 354 (1986).
[4] G. R. Satchler, Nucl. Phys. A **472**, 591 (1987).

[5] D. J. Hinde, M. Dasgupta, B. R. Fulton, C. R. Morton, R. J. Wooliscroft, A. C. Berriman, and K. Hagino, Phys. Rev. Lett. **89**, 272701 (2002).
[6] E. F. Aguilera *et al.*, Phys. Rev. C **63**, 061603(R) (2001).
[7] Y. W. Wu *et al.*, Phys. Rev. C **68**, 044605 (2003).
[8] N. Keeley *et al.*, Nucl. Phys. A **571**, 326 (1994).
[9] A. M. M. Maciel *et al.*, Phys. Rev. C **59**, 2103 (1999)
[10] J. Lubian *et al.*, Nucl. Phys. A **791**, 24 (2007).
[11] V. N. Garcia, J. Lubian, P. R. S. Gomes, A. Gómez-Camacho, and L. F. Canto, Phys. Rev. C **80**, 037602 (2009).
[12] L. F. Canto, J. Lubian, P. R. S. Gomes, and M. S. Hussein, Phys. Rev. C **80**, 047601 (2009).
[13] M. S. Hussein, P. R. S. Gomes, J. Lubian, and L. C. Chamon, Phys. Rev. C **73**, 044610 (2006).
[14] J. O. Fernández Niello *et al.*, Nucl. Phys. A **787**, 484c (2007).
[15] J. M. Figueira *et al.*, Phys. Rev. C **75**, 017602 (2007).
[16] J. M. Figueira *et al.*, Phys. Rev. C **81**, 024613 (2010).
[17] A. R. Garcia *et al.*, Phys. Rev. C **76**, 067603 (2007).
[18] A. M. Sanchez-Benitez *et al.*, Nucl. Phys. A **803**, 30 (2008).
[19] A. Gómez Camacho, E. F. Aguilera, E. Martinez-Queiroz, P. R. S. Gomes, J. Lubian, and L. F. Canto, Nucl. Phys. A **833**, 156 (2010).
[20] E. F. Aguilera *et al.*, Phys. Rev. C **79**, 021601(R) (2009).
[21] T. Udagawa, T. Tamura, and B. T. Kim, Phys. Rev. C **39**, 1840 (1989); T. Udagawa, B. T. Kim, and T. Tamura, *ibid.* **32**, 124 (1985).
[22] A. Gómez Camacho, E. F. Aguilera, and A. M. Moro, Nucl. Phys. A **762**, 216 (2005); A. Gómez Camacho, P. R. S. Gomes, J. Lubian, E. F. Aguilera, and I. Padrón, Phys. Rev. C **76**, 044609 (2007).
[23] P. R. S. Gomes *et al.*, Nucl. Phys. A **828**, 233 (2009).
[24] A. Gómez Camacho, P. R. S. Gomes, J. Lubian, and I. Padron, Phys. Rev. C **77**, 054606 (2008).
[25] P. R. S. Gomes *et al.*, Phys. Rev. C **70**, 054605 (2004).
[26] G. V. Marti *et al.*, Phys. Rev. C **71**, 027602 (2005).
[27] J. Lubian, I. Padron, P. R. S. Gomes, A. M. M. Maciel, R. M. Anjos, S. B. Moraes, J. J. S. Alves, C. Muri, R. Liguori Neto, and N. Added, Phys. Rev. C **64**, 027601 (2001).